

## Effect of amphiphilic copolymer containing ruthenium tris(bipyridyl) photosensitizer on the formation of honeycomb-patterned film

Bong Seong Kim, C. Basavaraja, Eun Ae Jo, Dae Gun Kim, Do Sung Huh\*

Department of Chemistry and Institute of Basic Science, Inje University, Obang 607 Gimhae City, Kyungnam 621-749, South Korea

### ARTICLE INFO

#### Article history:

Received 1 April 2010

Received in revised form

17 May 2010

Accepted 22 May 2010

Available online 2 June 2010

#### Keywords:

Amphiphilic polymer

Ruthenium tris(bipyridyl)

Honeycomb structure

### ABSTRACT

A new functional amphiphilic polymer ( $A_p$ ) containing ruthenium tris(bipyridyl) photosensitizer was synthesized and a honeycomb-patterned film was fabricated by casting a polystyrene solution and different concentrations of  $A_p$  under humid conditions. The amphiphilic copolymer was obtained by the radical copolymerization of ruthenium (4-vinyl-4'-methyl-2,2'-bipyridine)bis(2,2'-bipyridine)bis(hexafluorophosphate) with *N*-dodecylacrylamide and *N*-isopropylacrylamide. Without the addition of  $A_p$ , irregularly ordered porous films were obtained, while adding  $A_p$  in the casting solution resulted in highly ordered honeycomb-patterned films. In addition, the pore diameter and height of the porous structure increased with the increase of  $A_p$  amount in the solution. However, an excessive amount of  $A_p$  induced an irregularly structured pattern with small pore sizes.

© 2010 Elsevier Ltd. All rights reserved.

### 1. Introduction

Highly ordered porous polymer films have attracted much attention due to their potential applications in areas such as tissue engineering [1,2], photonic band gap [3], and optoelectronic devices [4]. Porous films with ordered structures have been fabricated by a variety of methods [5,6], including lithography [7] or soft lithography [8,9], the use of colloidal crystals [10,11], emulsions [12], self-assembled rod-coil copolymers [13,14], and microphase-separated block copolymers [15,16].

Recently, a simple method to create ordered structure porous films was introduced by Pitois et al. [17]. Highly ordered polymer films were produced by evaporating a solution of polymer dissolved in a volatile solvent under humid conditions. Water vapor condensed onto the cooling surface due to rapid solvent evaporation, then the droplets were trapped in the solution surface by surface tension. In order to help the trapping of water droplets in the hydrophobic solution surface, an amphiphilic copolymer is generally used in the polymer solution, because the polymer forms a stable monolayer at the air–water interface. Shimomura et al. have synthesized many kinds of neutral or ionic amphiphilic copolymers [18]. Among them, the best-known amphiphilic copolymer is obtained by the copolymerization of *N*-dodecylacrylamide and 6-hexanoic acid [19,20]; *N*-dodecylacrylamide acts as a hydrophobic while 6-hexanoic acid acts as a hydrophilic

component. Then, the polymers precipitated at the solution/water interface and effectively stabilized the droplets, thus preventing coalescence. The stabilized droplets were arranged in a well-ordered packing structure, induced by lateral capillary force and convection currents, which resulted from the temperature gradient in the solution. After the solvent and water completely evaporated, ordered traces (pores) were then obtained. These films have been fabricated from rod-coil block copolymers, polymers with ionic groups [21], amphiphilic copolymers [22], and star polymers [23,24].

Building and patterning inorganic nanoparticles into two- and three-dimensional organized structures by the manipulation of individual units is a potential route to the fabrication of chemical, optical, magnetic, and electronic devices with useful properties [25,26]. The synthesis and assembly of inorganic nanoparticles is currently an interesting issue. Composites formed from nanoparticles may possess unique applications in materials, such as batteries, electro-displays, molecular electronics, nonlinear optical materials, sensors, electromagnetic interference shielding, microwave absorption materials, and electrochromic devices [27–29]. Therefore, we introduce a new type of amphiphilic functional polymer including inorganic material of ruthenium.

Tris(2,2'-bipyridine)ruthenium(II) ion, or  $Ru(bpy)_3^{2+}$ , has received considerable attention from researchers because of its unique properties, such as strong luminescence, moderate excited-state lifetime, energy and electron transfer reactions, and chemical stability [30,31]. The luminescent excited state of  $Ru(bpy)_3^{2+}$  is assigned to the metal-to-ligand charge-transfer (MLCT) state. Luminescence properties are very sensitive to the

\* Corresponding author. Tel.: +82 55 320 3225; fax: +82 55 321 9718.

E-mail address: [chemhds@inje.ac.kr](mailto:chemhds@inje.ac.kr) (D.S. Huh).

polarity and viscosity of the solvent because of the MLCT characteristic. Therefore, fabrication of metallopolymer films with highly ordered structures containing  $\text{Ru}(\text{bpy})_3^{2+}$  is an important subject in the construction of electrochemical and photochemical devices [32].

Synthesizing a new type of amphiphilic functional polymer including  $\text{Ru}(\text{bpy})_3^{2+}$  and observing the effect of this polymer in the formation of honeycomb-patterned porous polymer films is induced by the consideration regarding on the possibility for the application of this polymer to overcome the limit of self-organizing process for the honeycomb pattern formation. To date, one major limitation in the formation of honeycomb-patterned

microstructures with the assistance of water-droplet is that the diameter/height ratio and interdroplet distance could not be separately controlled. This is because the formation of a highly ordered pattern by evaporation of a polymer solution dissolved in a volatile solvent under humid conditions is a self-organized process, though it can be controlled to achieve a narrow size distribution of the droplets [33]. It is difficult, however, to control the diameter/height ratio and interdroplet distance separately even if a stabilizing amphiphilic polymer for the regular package of water-droplet is used. An additional control factor is necessary to adjust the height/diameter ratio and interdroplet distance separately in self-organized microstructures.

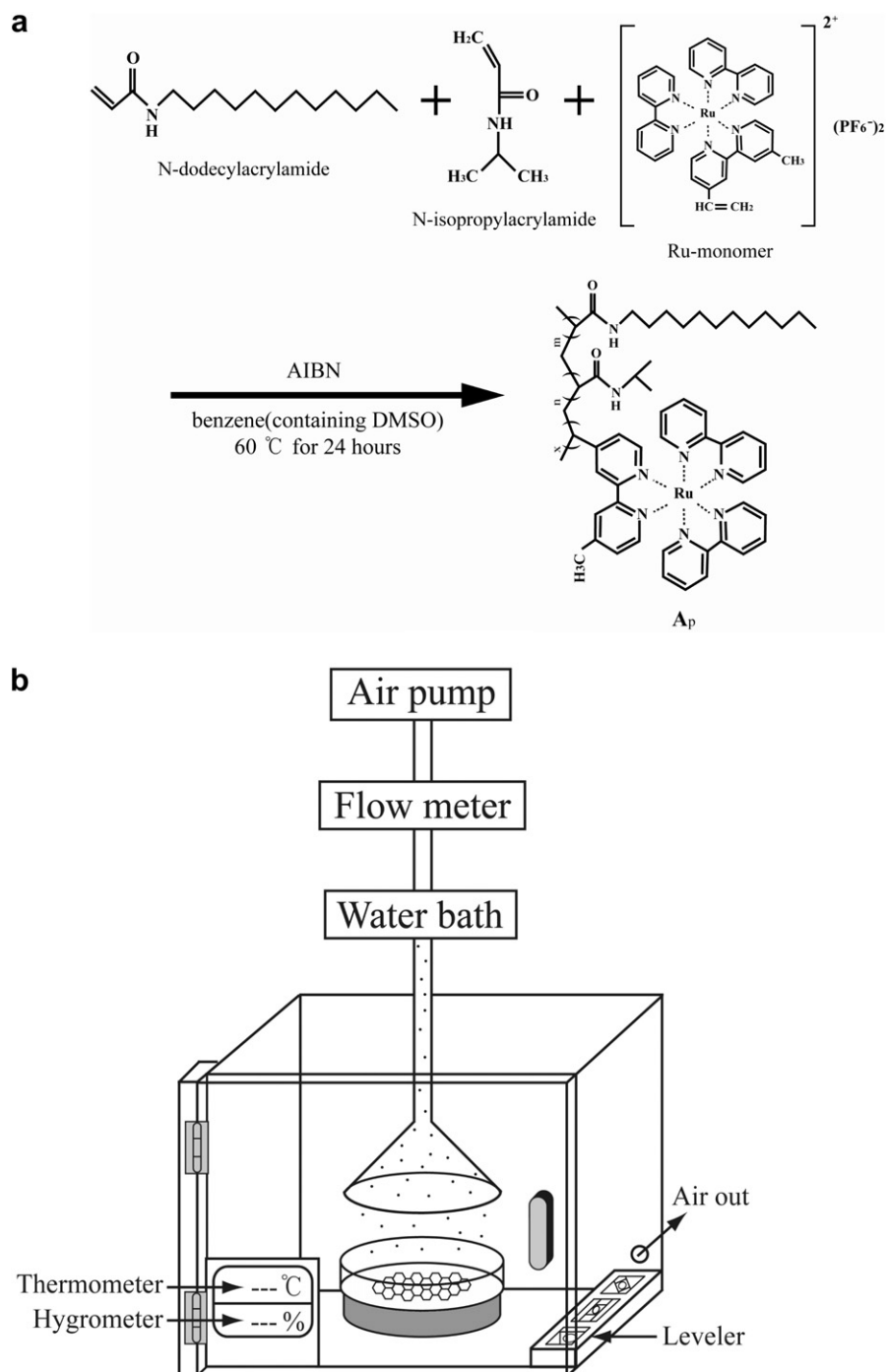


**Fig. 1.** (a) The scheme for the synthesis of  $\text{A}_p$  and (b) the overall experimental scheme for the pattern formation of honeycomb structure by the assistance of water-droplet.

This paper reports on the synthesis of a photo-active polymer containing  $\text{Ru}(\text{bpy})_3^{2+}$  and the fabrication of honeycomb-patterned-films depending on the added concentration of  $A_p$ . The film was obtained by a mixture of polystyrene and  $A_p$ . The  $A_p$  was synthesized by the radical copolymerization of ruthenium(4-vinyl-4'-methyl-2,2'-bipyridine)bis(2,2'-bipyridine)bis(hexafluorophosphate) (hereafter, referred to as Ru-monomer), *N*-dodecylacrylamide, and *N*-isopropylacrylamide. The synthesized copolymer was identified by UV-vis and Fourier Transform Infrared (FT-IR) spectroscopy. The morphologies of the honeycomb-patterned film were studied by varying the concentration of  $A_p$  in the polymer solution and then characterized by scanning electron microscopy (SEM).

## 2. Experimental

### 2.1. Materials

A polystyrene standard (PS, average  $M_w$  400,000  $\text{g mol}^{-1}$ ) was purchased from John Matthey Co. *N*-dodecylacrylamide was purchased from Tokyo Chemical Ind. *N*-isopropylacrylamide (97%), chloroform ( $\geq 99.8\%$ ), dimethyl sulfoxide (DMSO  $\geq 99.9\%$ ), benzene (99.8%), and

acetonitrile (99.8%) were all obtained from Aldrich Co. The initiator used for the copolymerization,  $\alpha, \alpha'$ -Azobis(isobutyronitrile) (AIBN), was purchased from Junsei Chemical Co. Ruthenium(4-vinyl-4'-methyl-2,2'-bipyridine)bis(2,2'-bipyridine)bis(hexafluorophosphate) was obtained from Fuji Molecular Planning Co.

### 2.2. Synthesis of amphiphilic polymer

*N*-dodecylacrylamide (8 mmol) and *N*-isopropylacrylamide (2 mmol) were dissolved in 27 mL benzene in a 4:1 ratio, respectively. To this solution, 2 mL DMSO containing 0.18 mmol Ru-monomer was added. The resulting solution was placed in a three-necked round bottom flask equipped with a thermometer, a nitrogen cock, and a reflux funnel, then stirred thoroughly to ensure an almost uniform media. To this mixture of monomers, 0.2 mmol AIBN was added to initiate the polymerization process. It was degassed with three freeze-evacuate-thaw cycles and, finally, the atmosphere was filled with dry nitrogen. Free-radical polymerization was conducted at 60 °C in an oil bath under nitrogen atmosphere for about 24 h. Acetonitrile was poured into the reaction mixture to precipitate the synthesized polymer. Polymer was collected by filtering and then washed in water to remove unreacted monomer. Finally, the product

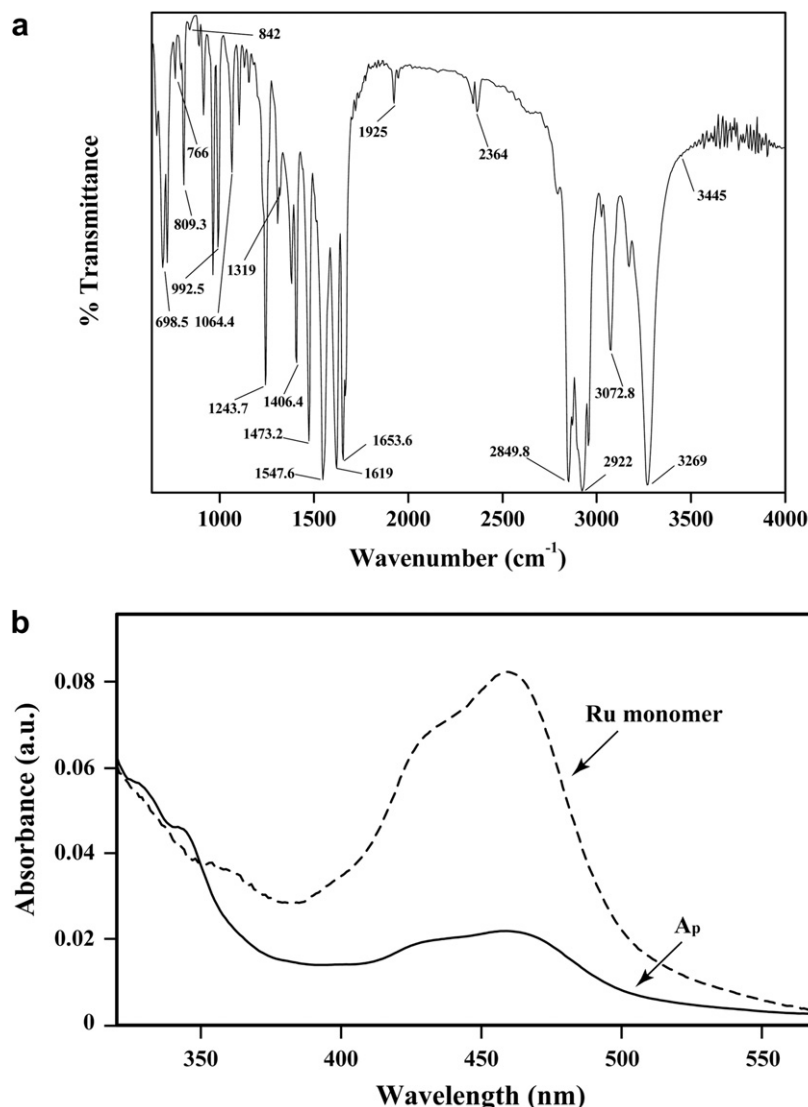


Fig. 2. (a) FT-IR spectra of the synthesized  $A_p$  polymer. (b) UV-Vis spectra of Ru-monomer and synthesized  $A_p$  polymer.

was dried *in vacuo*. The scheme for the synthesis of  $A_P$  is introduced in Fig. 1(a). The synthesized  $A_P$  polymer was further characterized by FT-IR and UV–vis spectroscopy to identify the type of interaction between the components of the polymer system. The infrared (IR) spectra of the polymer samples pelletized with KBr were obtained using an FT-IR spectrometer (Perkin–Elmer Model 1600). UV–vis spectra for Ru–monomer in water and  $A_P$  in chloroform were obtained by spectrometer (UVIKON-xs).

### 2.3. Fabrication of film

A solution of  $A_P$  and PS in chloroform was cast on a glass Petri dish. After complete evaporation of the solution under a humid condition, an opaque film was obtained. For a highly ordered honeycomb-patterned structure, evaporated water was applied on the solution surface through an air pump with a flow rate of 0.5 L/min. The microporous film was formed by the condensation and deposition of water droplets on the solution surface due to evaporative cooling. The obtained film structures were observed by optical microscopy (Olympus BX-51), and the images were processed into a computer by the image acquisition software (Motic Image Plus 2.0). A detailed pattern analysis was conducted using SEM (Philips XL-30 ESEM). Although the ratio of  $A_P$  composition varied, the total weight of PS and  $A_P$  was kept constant at 0.25 g in 4 mL chloroform. The solution was cast on a glass dish with

a diameter of 90 mm at a temperature of 20 °C and a relative humidity of 60%. The overall experimental scheme for the pattern formation of the honeycomb structure by the assistance of water-droplet is introduced in Fig. 1(b)

## 3. Result and discussion

### 3.1. Characterization of $A_P$ by FT-IR and UV–vis spectroscopy

Fig. 2(a) shows the FT-IR spectra for the new  $A_P$  polymer containing acrylamides and Ru–monomer. In the spectra, the absorption

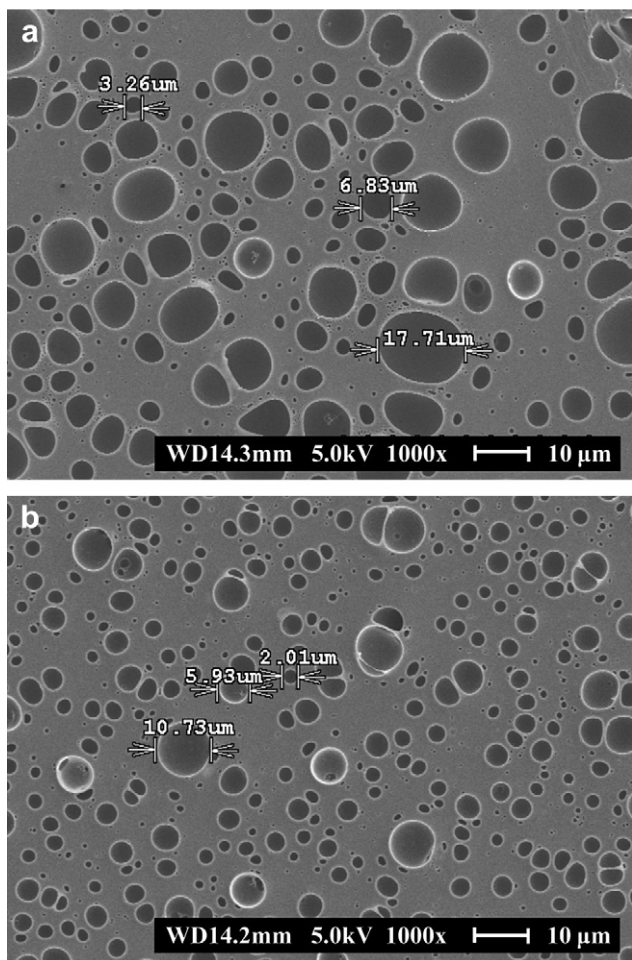


Fig. 3. SEM images of porous films prepared by casting solutions of PS without  $A_P$  by varying the PS concentration in the solution. (a) The concentration of PS is 0.25 g in 4 mL chloroform, while (b) is obtained by the half concentration of PS in the solution.

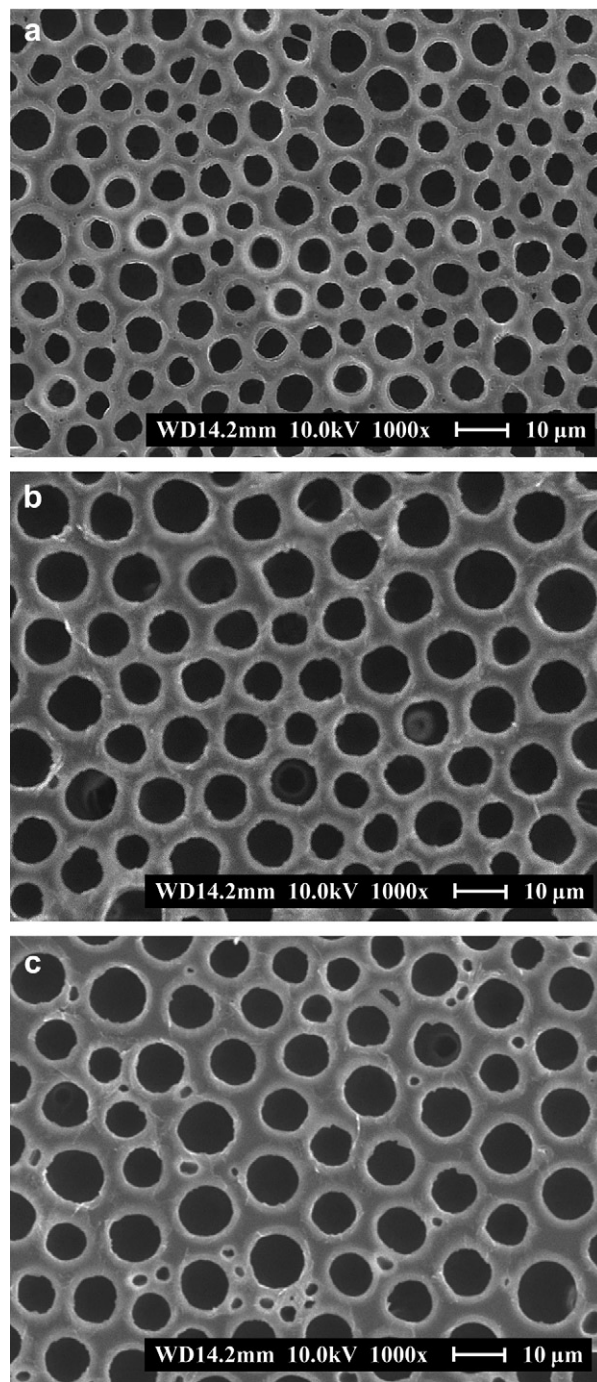


Fig. 4. SEM images of honeycomb pattern obtained by the addition of  $A_P$ , (a) the films by casting solutions of PS and  $A_P$  at a ratio of 9:1, (b) the films by casting solutions of PS and  $A_P$  at a ratio of 7:3, (c) the films by casting solutions of PS and  $A_P$  at a ratio of 5:5.



peak at  $3269\text{ cm}^{-1}$  can be attributed to the stretch for the hydrogen-bonded NH group. The antisymmetric stretching vibration of the  $\text{CH}_3$  group can be seen at  $2922\text{ cm}^{-1}$ . The  $\text{C}=\text{O}$  groups give rise to a strong band at  $1653.6\text{ cm}^{-1}$ . The mixed vibration of CN and NH appears at  $1319\text{ cm}^{-1}$ , and the antisymmetric deformation of  $\text{CH}_3$  is at  $1473.2\text{ cm}^{-1}$ . The double bands characteristic of the isopropyl group  $[-\text{CH}-(\text{CH}_3)_2]$  of  $\text{A}_\text{P}$  appear at  $1319$  and  $1406\text{ cm}^{-1}$ , and a peak at  $2922\text{ cm}^{-1}$  is observed due to the  $-\text{CH}-$  stretching vibrations of the  $-\text{CH}-$  bridges of the  $\text{A}_\text{P}$  network [34–36]. The other absorption bands at  $3445$ ,  $1243.7$ ,  $992.5$ ,  $842$ , and  $766\text{ cm}^{-1}$  correspond to the presence of the Ru-monomer in the polymer [32,37]. For *N*-dodecylacrylamide, absorption bands are also observed at  $992.5$ ,  $1243.7$ ,  $1406.4$ ,  $1619$ ,  $1653.6$ ,  $2850$ ,  $2922$ ,  $3073$ , and  $3269\text{ cm}^{-1}$  [38–40]. These peaks suggest a conjugation between the component

monomers of *N*-dodecylacrylamide, Ru-monomer, and *N*-isopropylacrylamide during the formation of  $\text{A}_\text{P}$  polymer. Fig. 2(b) shows the UV–vis spectra for the Ru-monomer and  $\text{A}_\text{P}$ . The absorption spectrum of the synthesized polymer of  $\text{A}_\text{P}$  derived from ruthenium trisbipyridine complex monomer also exhibits the characteristic metal-to-ligand charge-transfer band ( $^1\text{MLCT}-^1\text{A}_1$ ) centered at  $465\text{ nm}$ , analogous to Ru-monomer shown in this figure and other literature on  $\text{Ru}(\text{bpy})_3^{2+}$  [32,41].

### 3.2. The effect of $\text{A}_\text{P}$ on the honeycomb-patterned PS film

Fig. 3 shows the dewetting patterns investigated by SEM in the PS film formation without  $\text{A}_\text{P}$  in the physical conditions at  $20^\circ\text{C}$  and a relative humidity of 60% with an air flow rate of  $0.5\text{ L/min}$ . The

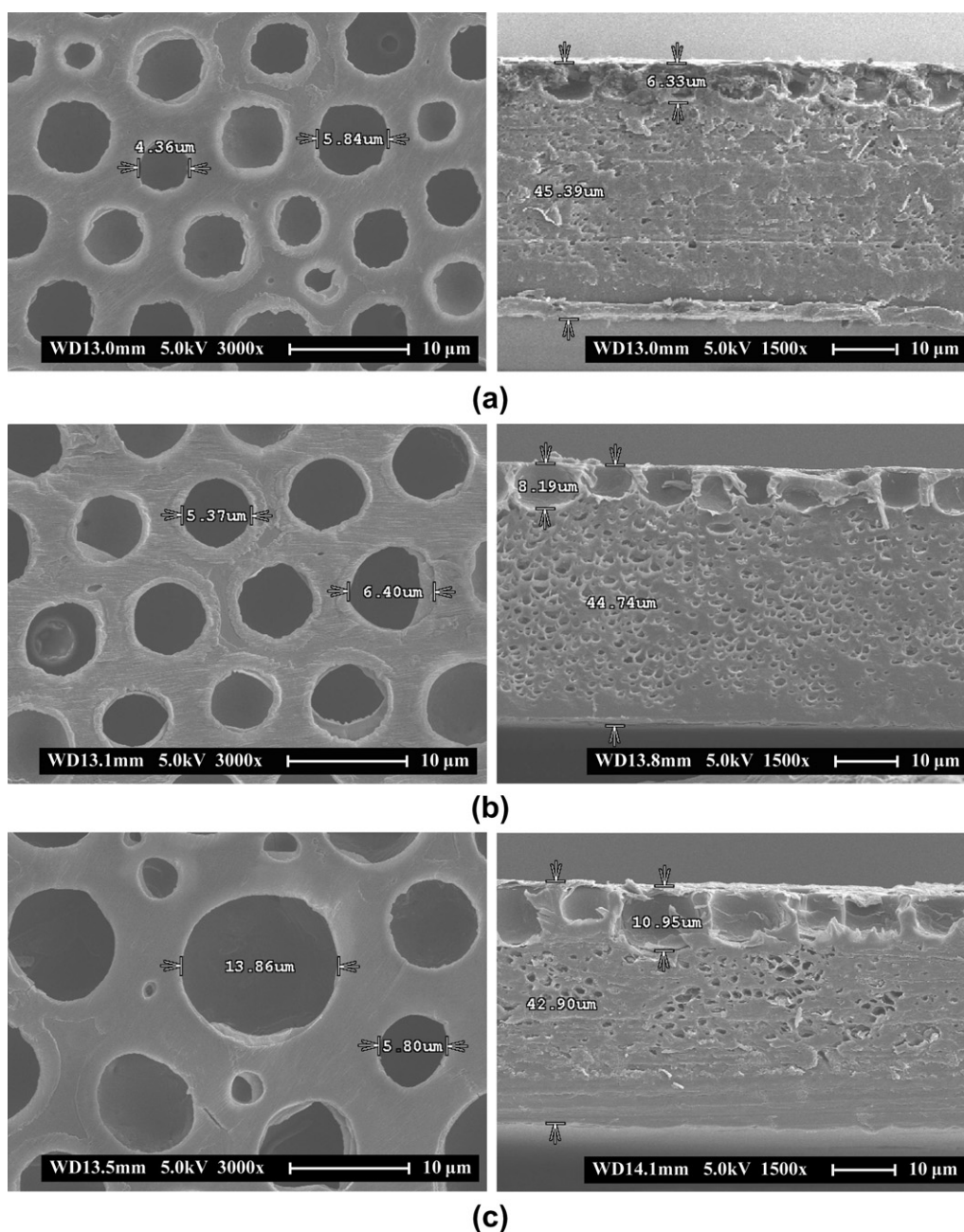


**Fig. 5.** SEM images showing a standard pore size depending on the concentration of  $\text{A}_\text{P}$ , (a) the films by casting solutions of PS and  $\text{A}_\text{P}$  at a ratio of 9:1, (b) the films by casting solutions of PS and  $\text{A}_\text{P}$  at a ratio of 7:3, (c) the films by casting solutions of PS and  $\text{A}_\text{P}$  at a ratio of 5:5. Left images indicate the surface image for diameter of the honeycomb structure and right images indicate the cross-sectional image for the pore height.

condition for Fig. 3(a) and (b) differs only at the PS concentration used in the solution. Fig. 3(a) is a typical image obtained at the PS concentration of 0.25 g in 4 mL chloroform, which corresponds to the amount kept constant in the presence of  $A_p$ , while Fig. 3(b) was obtained by using the PS as a half concentration, 0.125 g in 4 mL of chloroform. The reason for the comparison between Fig. 3(a) and (b) is in fact that the concentration of polymer (PS) itself is also an important factor affecting to the pattern formation. As shown in the image of Fig. 3(a), the pattern is irregular in both the hole size and the arrangement. Similar irregularity is also observed in the pattern with the half concentration of PS, as shown in Fig. 3(b), where the hole size is considerably smaller than that obtained in Fig. 3(a).

Fig. 4(a)–(c) shows typical honeycomb patterns obtained by the addition of  $A_p$  with weight percentages of 10, 30, and 50%, respectively. The images show regularly patterned honeycomb structures, indicating that the added  $A_p$  has a positive role for the formation of a patterned honeycomb structure in the fabrication of PS film. The solution systems with the weight percentage of 10% and 30% shown in Fig. 4(a) and (b) respectively are producing regularly patterned honeycomb structures, although the pattern shown in Fig. 4(c) obtained at 50% shows a little irregularity in the pattern, in which a small-sized pores appear between honeycomb structured pores. The small-sized pores arranging randomly indicates that an excessive amount of added  $A_p$  induces a negative effect for the formation of patterned honeycomb structure. The role of  $A_p$  as an amphiphilic polymer stabilizing the water-droplet for

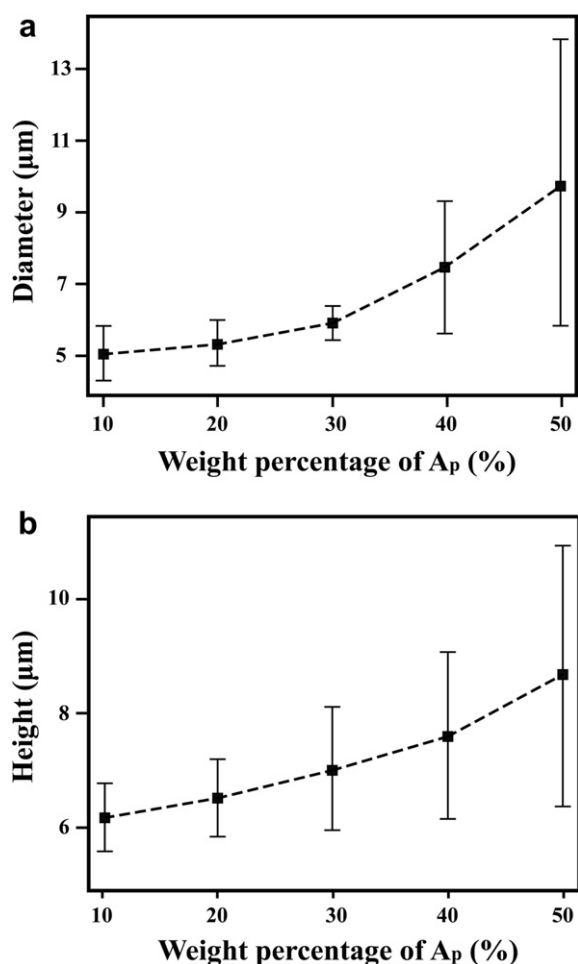


Fig. 6. Variation of pore size in the honeycomb structure depending on the concentration of  $A_p$ , (a) diameter depending on the concentration of  $A_p$ , and (b) height depending on the concentration of  $A_p$ .

Table 1

Diameter/height and interdroplet distance in the honeycomb structure depending on the concentration of  $A_p$ .

Honeycomb structure	Weight % of $A_p$		
	10%	30%	50%
Diameter/height	0.76–0.92	0.82–0.96	1.01–1.27
Interdroplet distance ( $\mu\text{m}$ )	3.51–4.80	4.22–5.32	2.11–5.87

the ordered honeycomb pattern could be distorted by adding an excessive amount of  $A_p$ , like a PS/ $A_p$  ratio of 1:1 (50%). The  $A_p$  is composed of *N*-dodecylacrylamide with a hydrophobic property and Ru-monomer with a hydrophilic property. The hydrophobic character will increase more than the hydrophilic character because *N*-dodecylacrylamide is a major component in  $A_p$ . It can be the reason why large- and small-sized pores are formed with a mixed pattern as shown in Fig. 4(c).

### 3.3. Dependence of pore diameter and height on the concentration of $A_p$

Fig. 5 shows the variations of standard pore diameter and height depending on the added concentration of  $A_p$ . As indicated in the left part of Fig. 5, the standard pore diameter in the honeycomb structure increases with an increase of  $A_p$  content in the polymer solution. However, a further increase in the concentration of  $A_p$  induces pores with a small diameter and a small distance apart, as shown in Fig. 5(c). The right part of Fig. 5 shows the variation of a standard pore height depending on the concentration of  $A_p$ . As shown in the figures, the pore height is also increased by the increase in the concentration of  $A_p$  proportional to the pore diameter. Fig. 6 presents a graphical diagram showing the dependence of pore size in the honeycomb structure on the weight percentage of  $A_p$ . The figure clearly shows the dependence of the diameter and height of the honeycomb pattern on the concentration of  $A_p$ , although a pattern with a uniform size is not obtained. A large range in Fig. 6(a) and (b) means a inhomogeneity of the pore size. This inhomogeneity increases with the increase in  $A_p$  content as mentioned in the previous section. Table 1 summarizes the standard ratios of diameter/height and interdroplet distance depending on the concentration of  $A_p$ . The table shows that the diameter/height ratio does not vary significantly by the concentration of  $A_p$ . However, the value increases slightly with the increase of  $A_p$ . Similarly, the interdroplet distance does not greatly depend on the weight percentage of  $A_p$ , but it is slightly increased by the increase in the concentration of  $A_p$ . It means there is a limit to controlling the self-organizing honeycomb pattern via the added amount of  $A_p$  alone, because the dependence of a standard diameter and pore height in the honeycomb pattern is also accompanied by variances in the interdroplet distance changing with a similar trend. However, the honeycomb pattern obtained by the assistance of water-droplet is significantly affected by the content of a new functional polymer of  $A_p$ . The  $A_p$  containing the cationic group of  $\text{Ru}(\text{bpy})_3^{2+}$  may adjust the hydrophilicity of the chains, which affect the facilitation of stabilization of the water droplets. An elaborate fabrication of photo-active polymer film with an ordered structure will therefore be possible using  $A_p$ .

## 4. Conclusion

In this paper, a new amphiphilic polymer ( $A_p$ ) including photosensitizer of  $\text{Ru}(\text{bpy})_3^{2+}$  is synthesized, and patterns on the surface of the microporous films are fabricated by the evaporation of a PS and an amphiphilic polymer solution under humid conditions. The concentration of  $A_p$  influences the honeycomb pattern

formation. The pore sizes grow larger in a particular range of the  $A_p$  content, whose role is to control the interfacial tension between water and polymer solution. The cationic charge of  $Ru(bpy)_3^{2+}$  in the Ru-monomer gives  $A_p$  high hydrophilicity. Therefore, the fabrication of polymer film into a highly ordered pattern with various structures using a photo-active metallopolymer, such as  $Ru(bpy)_3^{2+}$ , will be an important subject in the construction of electrochemical and photochemical devices.

## References

- [1] Shastri VP, Martin I, Langer R. *Proc Natl Acad Sci U S A* 2000;97(5):1970–5.
- [2] Nishikawa T, Nishida J, Ookura R, Nishimura SI, Wada S, Karino T, et al. *Mater Sci Eng C Biomim Mater Sens Syst* 1999;10:141–6.
- [3] Wijnhoven JEGJ, Vos WL. *Science* 1998;281:802–4.
- [4] Bolognesi A, Botta C, Yunus S. *Thin Solid Films* 2005;492(1–2):307–12.
- [5] Campbell M, Sharp DN, Harrison MT, Denning RG, Turberfield AJ. *Nature* 2000;404(6773):53–5.
- [6] Kim SH, Misner MJ, Xu T, Kimura M, Russell TP. *Adv Mater* 2004;16(3):226–31.
- [7] Whitesides GM, Grzybowski B. *Science* 2002;295:2418–21.
- [8] McDonald JC, Duffy DC, Anderson JR, Chiu DT, Wu H, Schueller OJA, et al. *Electrophoresis* 2000;21(1):27–40.
- [9] Odom TW, Love JC, Wolfe DB, Paul KE, Whitesides GM. *Langmuir* 2002;18(1):5314–20.
- [10] Kulinowski KM, Jiang P, Vaswani H, Colvin VL. *Adv Mater* 2000;12(11):833–8.
- [11] Imhof A, Pine DJ. *Nature* 1997;389(6554):948–51.
- [12] Jenekhe SA, Chen X. *Science* 1999;283:372–5.
- [13] Widawski G, Rawiso M, Francois B. *Nature* 1994;369(6479):387–9.
- [14] Lee M, Park MH, Oh NK, Zin WC, Jung HT, Yoon DK. *Angew Chem Int Ed* 2004;43(47):6465–8.
- [15] Thurn-Albrecht T, Steiner R, DeRouchey J, Stafford CM, Huang E, Bal M, et al. *Adv Mater* 2000;12(11):787–91.
- [16] Zalusky AS, Olayo-Valles R, Wolf JH, Hillmyer MA. *J Am Chem Soc* 2002;124(43):12761–73.
- [17] Pitois O, Francois B. *Colloid Polym Sci* 1999;277(6):574–8.
- [18] Maruyama N, Koito T, Nishida J, Sawadaishi T, Cieren X, Ijio K, et al. *Thin Solid Films* 1998;327–329:854–6.
- [19] Tsuruma A, Tanaka M, Fukushima N, Shimomura MJ. *Surf Sci Nanotech* 2005;3:159–64.
- [20] Yabu H, Shimomura M. *Langmuir* 2006;22:4992–7.
- [21] Karthaus O, Maruyama N, Cieren X, Shimomura M, Hasegawa H, Hashimoto T. *Langmuir* 2000;16(15):6071–6.
- [22] Kojima M, Hirai Y, Yabu H, Shimomura M. *Polymer J* 2009;41(8):667–71.
- [23] Lord HT, Quinn JF, Angus SD, Whittaker MR, Stenzel MH, Davis TP. *J Mater Chem* 2003;13(11):2819–24.
- [24] Conal LA, Gurr PA, Qiao GG, Solomon DH. *J Mater Chem* 2005;15(12):1286–92.
- [25] Korgel BA, Fitzmaurice D. *Adv Mater* 1998;10(9):661–5.
- [26] Mirkin C, Letsinger R, Mucic R, Storhoff J. *Nature* 1996;382(6592):607–9.
- [27] Yu C, Zhai J, Li Z, Wan M, Gao M, Jiang L. *Thin Solid Films* 2008;516(15):5107–10.
- [28] Cosa G, Chretien MN, Galletero MS, Fornes V, Gaecia H, Scanano JC. *J Phys Chem B* 2002;106:2460–7.
- [29] Yabu H, Tanaka M, Ijio K, Shimomura M. *Langmuir* 2003;19(15):6297–300.
- [30] Lai RY, Chiba M, Kitamura N, Bard AJ. *Anal Chem* 2002;74(3):551–3.
- [31] Singh P, Richter MM. *Inorg Chim Acta* 2004;357(5):1589–92.
- [32] Deronzier A, Jardon P, Martre A, Moutet JC, Santato C, Balzani V, et al. *New J Chem* 1998;22(1):33–7.
- [33] Karthaus O, Kiyono Y. *Jpn J Appl Phys* 2006;45(1B):588–90.
- [34] Sarac AS, Bardavit Y. *Prog Org Coat* 2004;49(2):85–94.
- [35] Percot A, Lafleur M, Zhu XX. *Polymer* 2000;41(19):7231–9.
- [36] Lin SY, Chen KS, Liang CR. *Polymer* 1999;40(10):2619–24.
- [37] Yoshida R, Yamaguchi T, Kokufuta E. *J Intel Mat Syst Str* 1999;10(6):451–7.
- [38] Nishida J, Nishikawa KA, Nishimura S, Wada S, Karino T, Nishikawa T, et al. *Polymer J* 2002;34(3):166–74.
- [39] Yabu H, Hirai Y, Shimomura M. *Langmuir* 2006;22(23):9760–4.
- [40] Li T, Chen J, Mitsuishi M, Miyashita T. *J Mater Chem* 2003;13(8):1565–9.
- [41] Khan SI, Beilstein AE, Sykora M, Smith GD, Hu X, Grinstaff MW. *Inorg Chem* 1999;38(17):3922–5.